Electronic Supplementary Material

Oxygen-deficient MoO_x/Ni_3S_2 heterostructure grown on nickel foam as efficient and durable self-supported electrocatalysts for hydrogen evolution reaction

Zihuan Yu[1], Haiqing Yan[1], Chaonan Wang[1], Zheng Wang,[1] Huiqin Yao (⌧)[2], Rong Liu (⌧)[3], Cheng Li (⌧)[4], Shulan Ma (⌧)[1]

1 Beijing Key Laboratory of Energy Conversion and Storage Materials, College of Chemistry, Beijing Normal University, Beijing 100875, China

2 School of Basic Medical Sciences, Ningxia Medical University, Yinchuan 750004, China

3 Analytical and Testing Center, Beijing Normal University, Beijing 100875, China

4 Shanghai Institute of Applied Physics, Chinese Academy of Sciences, Shanghai 201800, China

E-mails: huiqin_yao@163.com (Yao H); liur@bnu.edu.cn (Liu R); licheng@sinap.ac.cn (Li C); mashulan@bnu.edu.cn (Ma S)

Chemicals

All solvents and chemical reagents used in this work are analytical reagents and are used without further purification. Thiourea (CH_4N_2S) was acquired from Dingshengxin Chemical Reagent Co., Ltd in Tianjin. The nickel foam (NF, whose thickness is 1.6 mm and bulk density is 0.45 g cm^{-3}) was from Shenzhen Tianchenghe Technology Co. Ltd. Sodium molybdate dehydrate ($Na_2MoO_4·2H_2O$) was obtained from Bodi Chemical Reagent Co., Ltd in Tianjin. 5 wt% Nafion solution was got from Sigma-Aldrich Chemical Reagent Co., Ltd. Ethanol and sulfuric acid (H_2SO_4) were from Beijing Chemical Reagent Co., Ltd.

Characterization.

X-ray powder diffraction (XRD) patterns of the as-synthesized samples were obtained using a X pert pro MPD diffractometer (Cu Kα radiation, λ = 1.54056 Å), operating at 40 kV and 40 mA. The morphologies of the samples were inspected using field emission scanning electronic microscope (FESEM, S-8010, Hitachi) at an acceleration voltage of 10 kV and a high-resolution transmission electron microscope (HRTEM, JEM-2010, JEOL and FEI Technai G2 F20) at an acceleration voltage of 200 kV. X-ray photoelectron spectroscopy (XPS) spectra of the as-obtained products were collected using ESCALAB 250Xi spectrometer (Thermo Fisher) with Al-Kα X-ray as the radiation source. Raman spectra were carried out by using a microscopic confocal Raman spectrometer (LabRAM Aramis, Horiba Jobin Yvon) using a 633 nm He-Ne laser.

Electrochemical measurements

HER performance of all the catalysts was measured on the CHI 660E electrochemical workstation. Electrochemical impedance spectroscopy (EIS) was performed from 100 kHz to 0.01 Hz at -200 mV vs. RHE, with an AC amplitude of 5 mV. All potentials tested were calibrated to reversible hydrogen electrode (RHE) by the equation: $E_{(RHE)} = E_{(Ag/AgCl)} + 0.1976V + 0.0591\times pH$.

Calculation method

First-principles calculations was performed using density functional theory (DFT) [1] within project augmented wave method (PAW) [2] implemented in the Vienna ab initio Simulation Package (VASP) [3]. Exchange and correlation energy is performed by Perdue-Burke-Ernzerhof (PBE) [4] version of the generalized gradient approximation (GGA). A vacuum separation of 15 Å was performed to avoid periodic force. And the bottom seven layers of atoms are fixed to simulate the bulk properties. A plane-wave cutoff energy of 450 eV is efficient to guarantee the convergence of the total energy. The atoms are completely relaxed with force below than 0.03 eV/Å. The vacancy formation energy was defined by $E_{ads} = E(O_v) – E(perfect) + 1/2\ E\ (O_2)$, where $E(O_v)$ is the total energy of structure containing the O vacancy, and E(perferect) and

$E(O_2)$ are the energies of strture without vacancy and isolated O_2 gas, respectively.

Table S1. Average mass loading of catalysts on NF substrates.

Samples	Mass loading /mg cm^{-2}
MoO_x/Ni_3S_2/NF-01	2.87
MoO_x/Ni_3S_2/NF-11	2.92
MoO_x/Ni_3S_2/NF-21	2.94
MoO_3/NF	2.92
Pt-C/NF	2.92

Table S2. The simulated series resistance (R_s) and charge transfer resistance (R_{ct}) values based on the fitting models.

Samples	R_s /Ω	R_{ct} /Ω
MoO_x/Ni_3S_2/NF-11	2.10	6.51
com-MoO_3/NF	0.43	21.51
Pt-C/NF	2.16	2.82

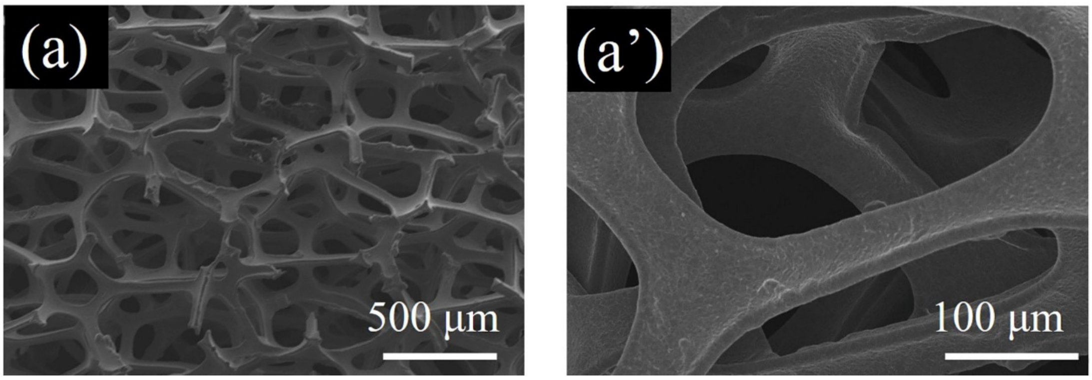

Fig. S1 SEM images of Ni foam (NF) at different magnification.

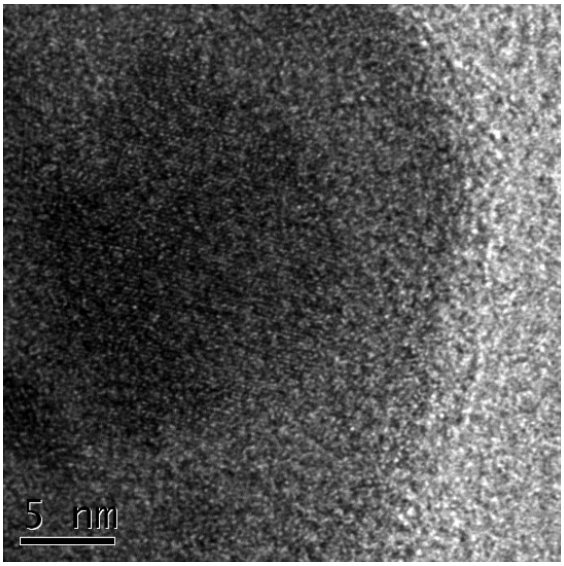

Fig. S2 Raw image (without scaling) of Fig 3c in the main text.

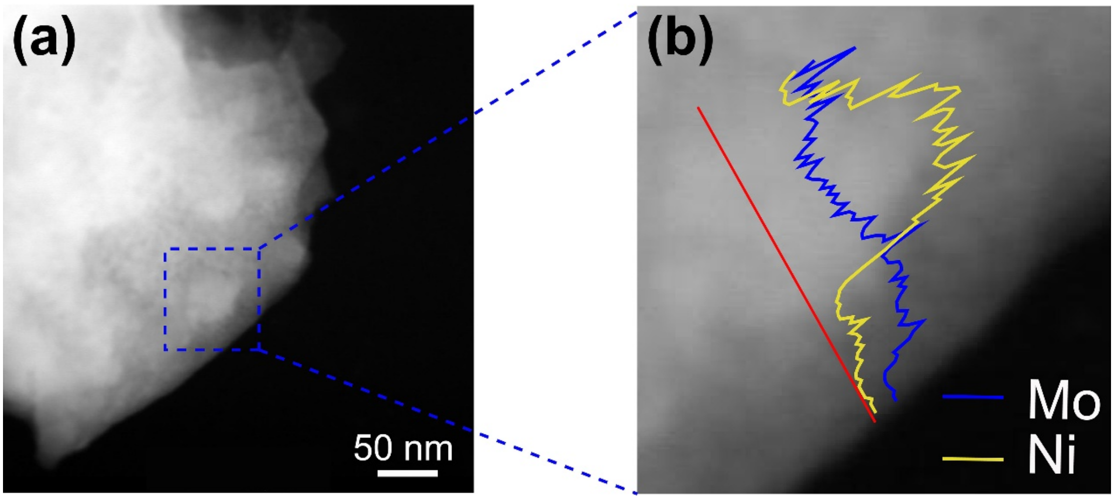

Fig. S3 (a) HAADF-STEM image of MoO_x/Ni_3S_2-11 and (b) corresponding line scans.

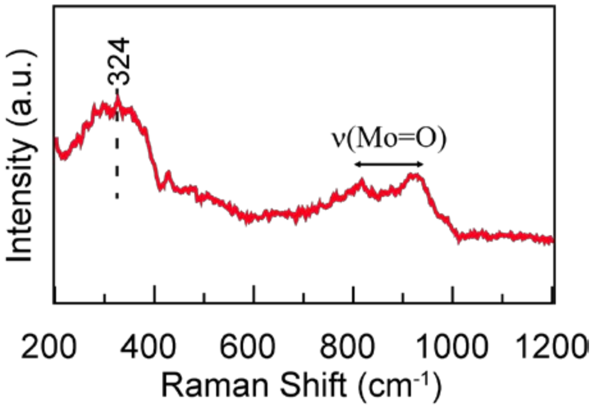

Fig. S4 Raman spectrum of MoO_x/Ni_3S_2/NF-11.

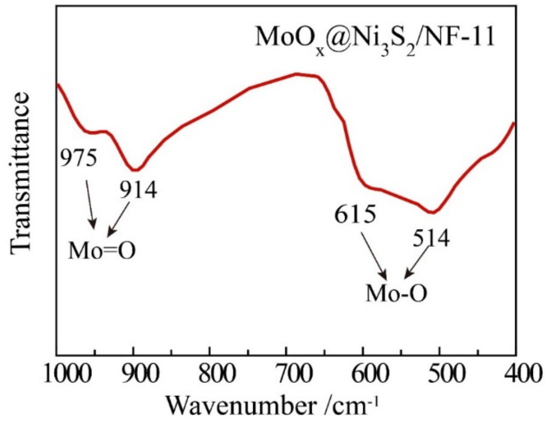

Fig. S5 FT-IR spectra of MoOx/Ni_3S_2/NF-11.

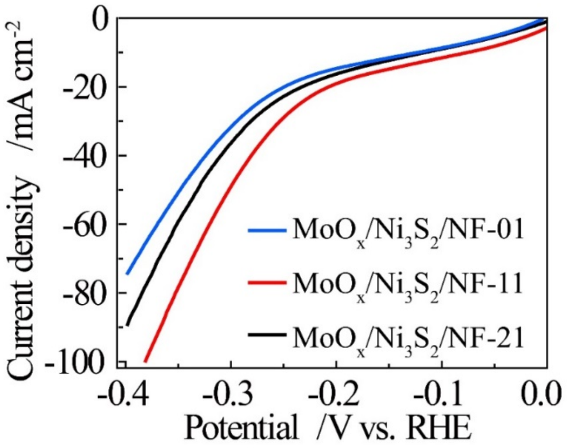

Fig. S6 Polarization curves of MoO_x/Ni_3S_2/NF-01, MoO_x/Ni_3S_2/NF-11, and MoO_x/Ni_3S_2/NF-21.

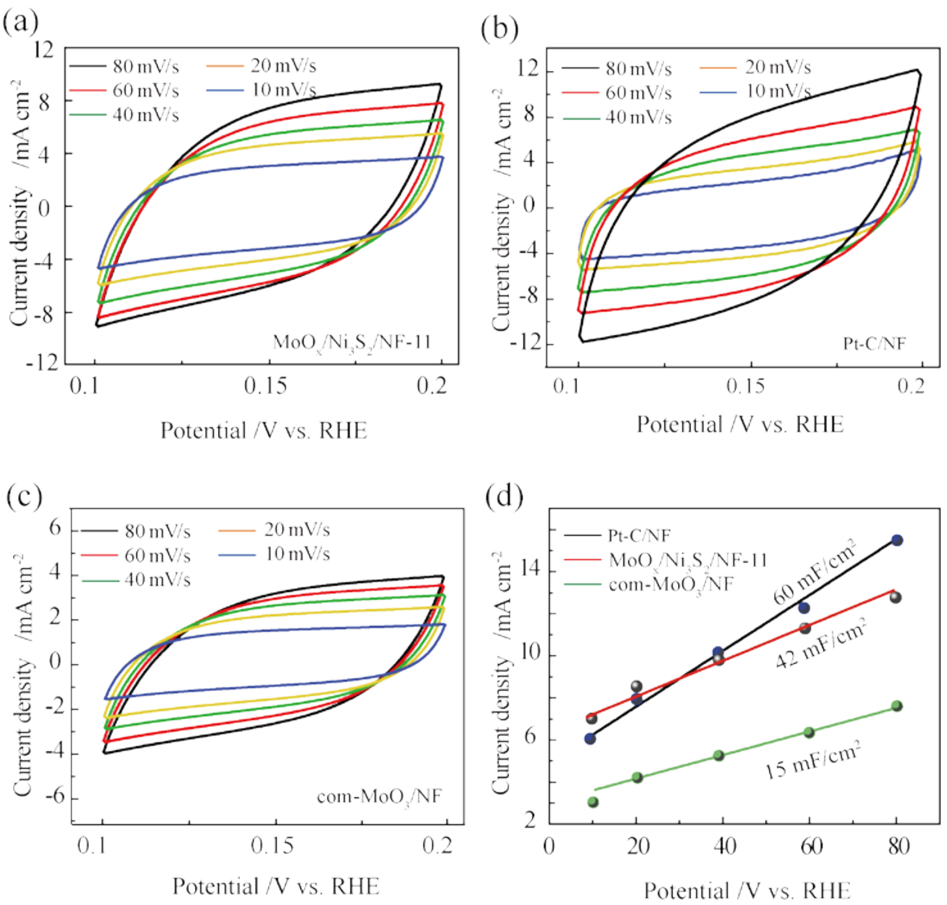

Fig. S7 Cyclic voltammetry curves of (a) MoO$_x$/Ni$_3$S$_2$/NF-11, (b) Pt-C/NF, (c) com-MoO$_3$/NF and (d) plots showing the extraction of the C_{dl}.

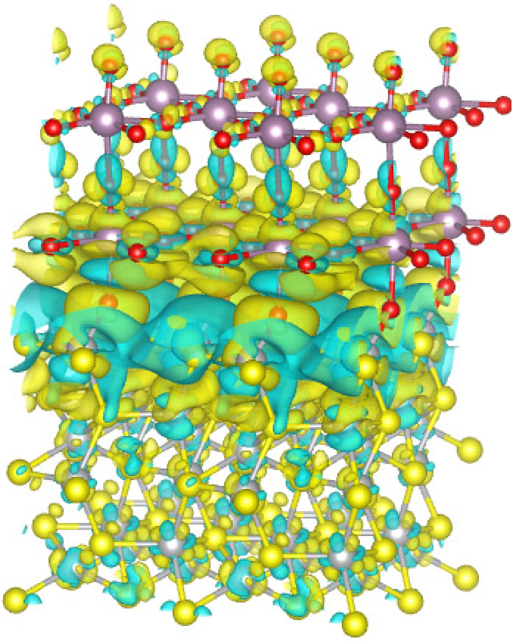

Fig. S8 The differential charge density distribution of MoO$_3$/Ni$_3$S$_2$ (without oxygen vacancy).

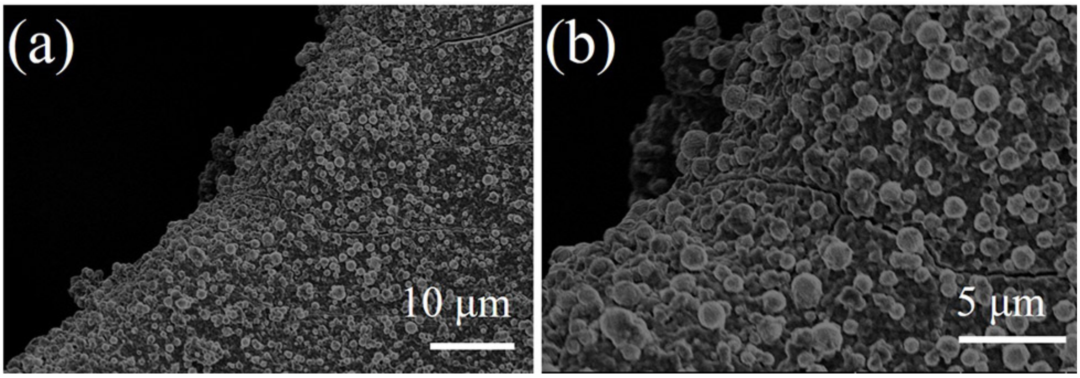

Fig. S9 SEM images of the sample after the 100 h stability test of MoO_x/Ni_3S_2/NF-11.

References

1. Kohn W, Sham L, Self-consistent equations including exchange and correlation effects. Physical Review, 1965, 140 (4A):A1133-A1138.
2. Blochl P, Projector augmented-wave method. Physical Review , 1994, 50(24): 17953-17979.
3. Kresse G, Furthmuller J, Efficient iterative schemes for ab initio total-energy calculations using a plane-wave basis set. Physical Review, 1996, 54(16): 11169-11186.
4. Perdew J, Burke K, Ernzerhof M, Generalized gradient approximation made simple. Physical Review Letters, 1996,77(18): 3865-3868.